Results in Engineering 17 (2023) 100915

Contents lists available at ScienceDirect

Results in Engineering

journal homepage: www.sciencedirect.com/journal/results-in-engineering

Research paper

Power flow methods used in AC distribution networks: An analysis of convergence and processing times in radial and meshed grid configurations

L.F. Grisales-Noreña [a,*], J.C. Morales-Duran [b], S. Velez-Garcia [c], Oscar Danilo Montoya [d,e], Walter Gil-González [f]

[a] Department of Electrical Engineering, Faculty of Engineering, Universidad de Talca, Curicó 3340000, Chile
[b] Departamento de Electrónica y Telecomunicaciones, Instituto Tecnológico Metropolitano, Medellín 050012, Colombia
[c] Departamento de Electromecánica y Mecratrónica, Instituto Tecnológico Metropolitano, Medellín 050012, Colombia
[d] Facultad de Ingeniería, Universidad Distrital Francisco José de Caldas, Bogotá D.C 110231, Colombia
[e] Laboratorio Inteligente de Energía, Universidad Tecnológica de Bolívar, Turbaco, Cartagena 131001, Colombia
[f] Department of Electrical Engineering, Facultad de Ingeniería, Universidad Tecnológica de Pereira, Pereira 660003, Colombia

ARTICLE INFO

Keywords:
Load flow
Power distribution system
Convergence analysis
Processing time
Meshed network
Radial network

ABSTRACT

The load flow problem (LFP) in power distribution networks allows us to find the nodal voltage values within the electrical systems. These values, along with the system parameters, are useful to identify the (technical, economic, and environmental) operational indices and constraints that describe the system's behavior under an established load scenario. The solution of the LFP requires the implementation of numerical methods due to its mathematical model's nonlinear and non-convex nature. In the specialized literature, multiple classical and modern methods seek to improve the solutions achieved in terms of convergence and processing times. However, the most efficient method in both radial and meshed networks has not been determined. Consequently, this study identified the most widely used and efficient classical and modern methods reported in the literature: Newton–Raphson (NR), Gauss-Seidel (GS), Iterative Sweep (IS), Successive Approximations (SA), Taylor's Series (TS), and Triangular Method (TM). The analysis also identified and selected the most common test scenarios to validate the effectiveness of the proposed solution methods: 10-, 33-, and 69-node systems in radial and meshed topologies. The software employed to validate the processing times and convergence of the numerical methods was MATLAB. The results obtained by the different methods were compared, taking the NR methodology as the base case. Thanks to its convergence, this method is used in commercial software packages to solve the LFP, as is the case of DIgSILENT. After analyzing the results of this study, we can state that all the selected methods were suitable in terms of convergence. The greatest errors were 6.064×10^{-07} for power losses and 8.017×10^{-04} for nodal voltages, which are negligible values for practical purposes in radial and meshed networks. In this work, processing time was employed as the selection criterion, and TM was identified as the most efficient method for solving the AC power flow in radial and meshed topologies for all the scenarios analyzed.

Nomenclature

δ	Voltage angles
$\mathbb{I}_d$	Currents demanded at the nodes
$\mathbb{I}_r$	Branch currents
$\mathbb{P}_i$	Active power injected into/demanded at node i
$\mathbb{Q}_i$	Reactive power injected into/demanded at node i
$\mathbb{S}_d^*$	Complex power demanded
$\mathbb{S}_g^*$	Complex power generated
$\mathbb{S}_i^*$	Net complex power injected into node i
$\mathbb{T}$	Triangular matrix
$\mathbb{V}$	Voltage magnitude
$\mathbb{V}_d$	Complex voltage at the demand nodes
$\mathbb{V}_i^*$	Complex voltage at node i
$\mathbb{V}_j$	Complex voltage at node j
$\mathbb{V}_n$	Nodal voltage
$\mathbb{V}_r$	Branch voltage
$\mathbb{V}_s$	slack node voltage

* Corresponding author.
E-mail addresses: luis.grisales@utalca.cl (L.F. Grisales-Noreña), juanmorales288981@correo.itm.edu.co (J.C. Morales-Duran), sebastianvelez@itm.edu.co (S. Velez-Garcia), odmontoyag@udistrital.edu.co (O.D. Montoya), wjgil@utp.edu.co (W. Gil-González).

https://doi.org/10.1016/j.rineng.2023.100915
Received 4 October 2022; Received in revised form 21 November 2022; Accepted 23 January 2023
Available online 26 January 2023

$\mathbb{Y}_{bus}$	Admittance matrix of the system that represents the lines and impedances connected to the nodes
$\mathbb{Y}_{ds}$	Subcomponent of the admittance matrix that connects the *slack* and demand nodes
$\mathbb{Y}_{ij}$	Component of the admittance matrix that interconnects nodes i and j
$\mathbb{Z}_{dd}$	Impedance matrix
$\mathbb{Z}_r$	Branch impedance matrix
A_d	Incidence matrix of the demand node
A_s	Incidence matrix of the slack node
J	Jacobian matrix
t	Iteration counter

Acronyms

CREG Energy and Gas Regulation Commission
LFP Load Flow Problem
NR Newton–Raphson
GS Gauss–Seidel
SA Successive Approximations
IS Iterative Sweep
TM Triangular Method
TS Taylor's Series
AC Alternating Current
p.u Per unit

1. Introduction

The power generation and consumption process involve some intermediate stages that enable the power to be transported from large generators to consumption points [1]. First, transmission networks operate at extra-high voltage levels, thus reducing electrical losses over long distances [2]. Then, there are the distribution networks, which receive power from the distribution substations fed by the transmission networks and deliver it to end users at lower voltage levels (CREG levels 1 and 2).

Due to the variability in power generation and demand within multinode electricity systems, it is necessary to identify a tool to assess the impact of various power generation and demand levels on the system's electrical variables: nodal voltages and line currents. The objective is to evaluate the technical, economic, and environmental indicators of the network proposed by the operator, as well as the technical constraints associated with the operation of electrical power systems (e.g., bounds in the nodal voltage profiles, and line currents, line loadability, power loss levels, among others) [3–5]. Such a tool is known as load flow.

It is worth mentioning that the mathematical formulation of the LFP has no analytical solution due to the nonlinearity of the system of equations. Therefore, it must be solved using numerical methods [6], many of which have been proposed over the last decades to address the problem in both meshed and radial AC networks. Said methods include GS [7], [8], NR [8], [9], IS [10], SA [11], linear approximations or TS [12], among others, which are evaluated in different test scenarios and compared with other methods to determine their effectiveness in terms of convergence and, in some cases, processing times. Such methods also guarantee the results' reliability by controlling the problem solution's convergence process so that the solution adequately represents the analyzed phenomenon. This, in turn, confirms that the results achieved by using the load flow tool to evaluate the operation of systems is an efficient operation and planning projects represent in a good way the real behavior of the system [13,14].

In addition, due to the high computational cost involved in implementing numerical methods to solve the LFP in power distribution, efficient solution strategies have been promoted in the literature to reduce computation times [3]. The above aims to evaluate the greatest number of possible scenarios as part of the efficient planning and operation strategies of the power distribution system within the times stipulated by the different power projects.

In the specialized literature, many authors have focused their attention on demonstrating the effectiveness of their strategies both in terms of solution quality and processing times. However, in many cases, they do not properly compare them with the most widely used classical methods or with recently reported efficient techniques [3]. Moreover, the studies use different test systems and computer equipment, which makes it difficult to determine the actual performance of the proposed methods. In this regard, this investigation found that no analyses for the selection of load flow methods have been reported in the literature. Such analyses should examine the convergence and computation times for both radial and meshed networks in order to identify the most efficient methodology for each type of topology existing within the AC networks.

Based on the current needs identified in state of the art, the purpose of this document is to evaluate the methods proposed in the specialized literature and, subsequently, select the most efficient one for solving the LFP in power distribution systems in terms of convergence and computation time both for meshed and radial networks. To this end, the most widely used and efficient methods reported in recent years were selected. Then, radial and meshed configurations of different sizes were used to assess the efficiency of each method in the various topologies existing within the networks. Under real operation conditions, some electrical systems may present both meshed and radial topologies during different operating times. This can be caused by the activation of protective devices trying to reconnect fractions of the system in the event of faults [15]. Consequently, this paper also analyzes the effect of the selected load flow methods on networks that can operate with both configurations.

The main contributions of this paper are as follows: (i) a single document that consolidates the formulation and convergence process of the main methods for solving the LFP in radial and meshed networks; (ii) a statistical methodology to assess the efficiency of the load flow methods in terms of convergence and processing times; and (iii) the identification of the most efficient LPF method for addressing radial and meshed distribution networks.

The rest of this paper is organized as follows. Section 2 introduces the mathematical formulation of the different methods selected to solve the LFP in radial and meshed AC networks. Section 3 describes the various test systems and their characteristics (i.e., line resistances, reactances, and active and reactive power demanded at each node, among others). Section 4 reports the results of the simulations carried out by each solution method in each test scenario, including comparative analyses. Finally, Section 5 draws the conclusions of the study and proposes future research lines.

2. Mathematical formulation and power flow methods

2.1. Power flow problem formulation

The LFP is a nonlinear and nonconvex problem that seeks to determine the voltages and angles of all the busbars in the system in order to analyze their impact on the technical and operating conditions of the network under a constant power scenario for a specific period of time (static analysis). To this end, a set of nonlinear algebraic equations should be solved, which, per node, comprise six variables: voltage magnitude, its respective angle, and the active and reactive power generated and demanded. Solving such equations allows us to determine active and reactive power losses, voltage regulation in the system, static voltage stability characteristics, reactive compensation, and power flow through the lines, among other elements [16].

$$\mathbb{S}_i^* = \mathbb{V}_i^* \sum_{j=1}^{n} \mathbb{Y}_{ij} \mathbb{V}_j \tag{1}$$

Eq. (1) shows the overall power balance in an electrical system. It is used to represent the LFP, where ($\mathbb{S}_i^*$) is the conjugate of the net power injected at node i, ($\mathbb{Y}_{ij}$) is the admittance matrix that describes the connections of nodes i and j, ($\mathbb{V}_i^*$) is the conjugate of the voltage at node i, ($\mathbb{V}_j$) is the voltage at node j, and n is the number of nodes in the system. This equation can also be expressed as shown in Eq. (2). In this case, ($\mathbb{S}_g^*$) is the conjugate of the generated power and ($\mathbb{S}_d^*$) is the conjugate of the demanded power.

$$\mathbb{S}_i^* = \mathbb{S}_g^* - \mathbb{S}_d^* = diag\left(\mathbb{V}^*\right)\mathbb{Y}_{bus}\mathbb{V} \tag{2}$$

The nodal voltages of the system are the variables to be found by solving the above nonlinear equation. Additionally, the LFP identifies the active and reactive powers to be injected by the slack generator. It is worth mentioning that this study focuses on power distribution networks; it does not consider PV nodes or their variables. Furthermore, due to the nonlinearities of this equation, it cannot be solved analytically and requires the application of numerical methods.

2.2. Power flow methods

In the literature, we can find multiple numerical methods to solve the LFP, which can be classified into two groups: derivative-based methods and derivative-free methods [17]. This study selected two classic methods (NR and GS) and four modern methods (SA, IS, TM, and TS, published over the last three years) in order to validate their efficiency in solving the LFP in radial and/or meshed networks. This selection was based on the wide implementation of these methodologies in the literature (in the case of the classical methods) and on the excellent results in terms of convergence and processing times reported by the researchers.

The mathematical formulations of each selected method are presented below. However, we also recommend reviewing the references provided in each case for a better understanding.

2.2.1. Newton–Raphson (NR)

The formulation of this classical solution method is based on the Jacobian matrix (J), which provides a linear relationship between the small changes in voltage angle (δ) and magnitude ($\mathbb{V}$) and the small variations in active (ΔP_i) and reactive (ΔQ_i) power [9].

To obtain the recursive formula of the NR method, an iteration counter (t) is added. Said formula can be observed in Eq. (3). This equation starts with typical plane voltages (nodal voltages to $1\angle 0$ in p.u) and iterates until converging to a convergence error set for the problem. This applies to all the methods that employ iterative processes to solve the LFP, which is the case of all the methods used in this paper.

$$\begin{bmatrix}\Delta P_i^t \\ \Delta Q_i^t\end{bmatrix} = [J]\begin{bmatrix}\delta_i^{t+1} - \delta_i^t \\ \mathbb{V}_i^{t+1} - \mathbb{V}_i^t\end{bmatrix}. \tag{3}$$

2.2.2. Gauss–Seidel (GS)

It is a classical load flow method that reorganizes Eq. (1) in terms of $\mathbb{V}_i$, using the mathematical basis of the Gauss-Seidel methodology to solve the LFP. The result of this reorganization is shown in Eq. (4), where an iteration counter (t) is also added to make the recursive equation [9], [18].

$$\mathbb{V}_i^{t+1} = \frac{1}{\mathbb{Y}_{ii}}\left(\frac{P_i - jQ_i}{\mathbb{V}_i^{t,*}} - \sum_{j<i}^{n}\mathbb{Y}_{ij}\mathbb{V}_j^{t+1} - \sum_{j>i}^{n}\mathbb{Y}_{ij}\mathbb{V}_j^{t}\right). \tag{4}$$

This method updates the nodal voltages in an ordered way by using, in every nodal voltage, all the previous updated voltages, which improves its efficiency in terms of convergence and processing times when compared to the Gauss method. [16].

2.2.3. Successive approximations (SA)

It is an open numerical method employed to solve the LFP, which seeks to find the roots of an equation. It does not require an interval that brackets a root but a starting value close to it. A derivative-free formulation is implemented to carry out the iterative process and find its solution (where the solution time is proportional to the proximity between the starting and root values). Given that it does not require the inverse of nondiagonal matrices for each iteration, it helps reduce the computation time.

$$\mathbb{V}_d^{t+1} = -\mathbb{Z}_{dd}[\mathbb{Y}_{ds}\mathbb{V}_s + diag^{-1}(\mathbb{V}_d^{t,*})\mathbb{S}_d^*]. \tag{5}$$

Eq. (5) describes the iterative process of the SA method, which seeks to find the complex conjugate voltage at the demand nodes ($\mathbb{V}_d$). However, this process requires the addition of an iteration counter (t) to obtain these values, taking as a starting point a value that is usually the slack node voltage ($\mathbb{V}_s$). The minus sign (-) refers to the power output of the distribution system. In this equation, ($\mathbb{Z}_{dd}$) represents the inverse of the admittance matrix, also known as the impedance matrix. Said inversion is done to avoid calculating the inverse iteratively. Although some subcomponents of the admittance matrix are still required and are represented by ($\mathbb{Y}_{ds}$), they only consider the interconnection between the slack node and the demand nodes. Lastly, this equation also takes into account the complex conjugate power demanded from the demand nodes ($\mathbb{S}_d^*$).

2.2.4. Iterative sweep (IS)

Also known as the backward/forward method, it has a derivative-free formulation that employs an iterative counter (t) very similar to the one described in the SA method. However, in this case, differentiating between the nodal ($\mathbb{V}_n$) and branch ($\mathbb{V}_r$) voltages in the distribution system under study is fundamental. Moreover, the directions of the currents flowing through the lines must be assumed, and their effects are represented by an incidence matrix of the node–branch type (A). This shows that the branch voltages are equal to the transpose of the incidence matrix times the nodal voltages. However, this incidence matrix is, in turn, divided into two parts, slack node (A_s) and demand nodes (A_d), so that the resulting iterative equation can be expressed in terms of ($\mathbb{V}_d$). Finally, considering that the currents demanded at the nodes ($\mathbb{I}_d$) are equal to the product of (A_d) times the branch currents ($\mathbb{I}_r$), and applying Ohm's law to the branches, it is possible to obtain the branch impedances ($\mathbb{Z}_r$) presented in Eq. (6). This equation describes the iterative process of the iterative sweep method.

$$\mathbb{V}_d^{t+1} = -\left(A_d\mathbb{Z}_r^{-1}A_d^T\right)^{-1}\left[diag^{-1}\left(\mathbb{V}_d^{t,*}\right)\mathbb{S}_d^* + A_d\mathbb{Z}_r^{-1}A_s^T\mathbb{V}_s\right]. \tag{6}$$

2.2.5. Triangular method (TM)

The original formulation of this method only allows for solving the power flow in radial distribution systems [19,20]. However, with the modifications proposed by [21,22], it is possible to analyze radial and meshed topologies. This method has many similarities with the IS method, as it involves a derivative-free formulation, requires differentiating between the branch and nodal voltages, and needs an additional matrix to be solved. The IS method uses the incidence matrix, while the TM requires a triangular matrix (T) that represents the nodal currents transported by the currents of each of the branches. This matrix is so named because of its shape, as all of its components are located at the top of the diagonal of the matrix. The iterative process of the TM is represented by Equation (7). In addition, it offers reduced computation times because ($T^T\mathbb{Z}_rT$) is calculated only once and not at every iteration.

$$\mathbb{V}_d^{t+1} = \mathbb{V}_s + T^T\mathbb{Z}_rT\,diag^{-1}\left(\mathbb{V}_d^{t,*}\right)\mathbb{S}_d^*. \tag{7}$$

Remark. The upper-triangular power flow method can be applied to meshed distribution networks with only one slack bus by using a loop-based analysis approach, as presented by the authors of [22]. The work by [21] presents complete details regarding the reformulation of Equation (7) in order to make it compatible with meshed distribution networks.

2.2.6. Taylor's series (TS)

This load flow method linearizes the hyperbolic relation between voltages and powers by using the complex Taylor series expansion [17],[23]. Eq. (8) is the recursive formula that represents the TS method [17],[23], where the subscripts $\mathfrak{R}$ and $\mathfrak{I}$ refer to the real and imaginary part, respectively.

$$\begin{bmatrix} V_{\mathfrak{R}}^{t+1} \\ V_{\mathfrak{I}}^{t+1} \end{bmatrix} = \begin{bmatrix} A_{\mathfrak{R}}^{t} + B_{\mathfrak{R}}^{t} & A_{\mathfrak{I}}^{t} - B_{\mathfrak{I}}^{t} \\ A_{\mathfrak{I}}^{t} + B_{\mathfrak{I}}^{t} & B_{\mathfrak{R}}^{t} - A_{\mathfrak{R}}^{t} \end{bmatrix}^{-1} \begin{bmatrix} C_{\mathfrak{R}}^{t} \\ C_{\mathfrak{I}}^{t} \end{bmatrix}. \tag{8}$$

Eq. (9) shows the equivalences of the complex square matrices of A and B, as well as of the complex vector of C [23].

$$\begin{aligned} A &= diag^{-2}(\mathbb{V}_d^{0,*})diag(\mathbb{S}_d^{*}), \\ B &= -\mathbb{Y}_{dd}, \\ C &= -(2diag^{-1}(\mathbb{V}_d^{0,*})diag(\mathbb{S}_d^{*}) + \mathbb{Y}_{ds}\mathbb{V}_s). \end{aligned} \tag{9}$$

Finally, the iterative process to be performed to solve the LFP using the methods previously described is represented by the following algorithm:

Data: Load the radial or meshed system data;
Load the vectors and matrices that make up each algorithm;
Load the v_0, v_d^t (with $t = 0$), ϵ, and t_{max} data;
for $t = 0 : t_{max}$ **do**
  Evaluate the proposed iterative equation for each method;
  if $max\left(\left|v_d^{t+1} - v_d^t\right|\right) \leq \epsilon$ **then**
    Solution achieved;
    Result: Return $v_d = v_d^{t+1}$.
    break;
  else
    $v_d^{t+1} = v_d^t$;
  end
end

Algorithm 1: Proposed iterative algorithm for evaluating each of the solution methods.

Algorithm 1 outlines the iterative solution strategy implemented with each solution algorithm. Initially, the (radial or meshed) system data are loaded. Then, the vectors and matrices (necessary to calculate the voltages using the different algorithms selected) are loaded. These data are clearly detailed within each of the source documents of the algorithms. Subsequently, the initial data of the problem are loaded: initial nodal voltages v_0, demand voltages at iteration t (v_d^t with $t = 0$), selected convergence error ϵ, and the maximum number of iterations of the iterative algorithm t_{max}. After loading these data, the iterative process starts and, iteration by iteration assesses the load flow function proposed for each solution method, as well as the convergence of the algorithm. When the expected convergence level is reached, the algorithm stops and returns the nodal voltage data of the analyzed system, thus ending the iterative process. If the level is not reached, the voltages at the demand nodes are updated, and the iterative process continues until achieving the maximum number of iterations.

3. Test systems and considerations

This section presents the test systems used and the considerations taken into account for the analyses made in this study.

3.1. 10-node test system

This section describes the electrical configuration and the main parameters of the radial and meshed 10-node systems. The radial version of this system consists of 10 nodes and 9 lines, with base voltage and power of 23 kV and 100 kW, respectively. The electrical configuration of the system is illustrated in Fig. 1.

Table 1 summarizes the main parameters for simulation and validation. It includes, from left to right, the sending node, the receiving node, the interconnection resistance between the sending and receiving nodes ($R_{ij}[\Omega]$), the reactance associated with it, ($X_{ij}[\Omega]$), and the active (kW) and reactive (kVar) power demanded at each of the receiving nodes. This test system was adapted from Grisales-Noreña et al. [24], and Garces [25]. In this study, all the tables that describe the parameters of the meshed and radial versions follow the same format described above.

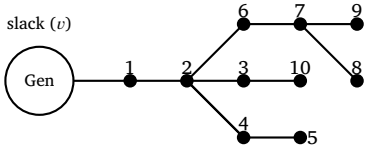

Fig. 1. 10-node radial topology.

Table 1
Electrical parameters of the 10-node radial topology.

Node i	Node j	$R_{ij}[\Omega]$	$X_{ij}[\Omega]$	$P_j[kw]$	$Q_j[kVar]$
1	2	0.1233	0.4127	1840	460
2	3	0.2467	0.6051	980	340
2	4	0.7469	1.2050	1790	446
4	5	0.6984	0.6084	1598	1840
2	6	1.9837	1.7276	1610	600
6	7	0.9057	0.7886	780	110
7	8	2.0552	1.1640	1150	60
7	9	4.7953	2.7160	980	130
3	10	5.3434	3.0264	1640	200

Table 2
Electrical parameters added to obtain the 10-node meshed topology.

Node i	Node j	$R_{ij}[\Omega]$	$X_{ij}[\Omega]$	$P_j[kw]$	$Q_j[kVar]$
5	10	0.1426	0.4522	1640	200
8	10	0.2018	0.5214	1640	200

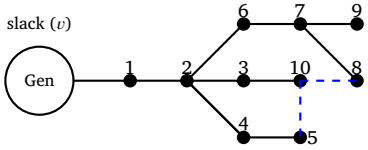

Fig. 2. 10-node meshed topology.

To obtain the 10-node meshed system, two connection lines were added to the 10-node radial topology described above, which are shown in blue in Fig. 2. This test system was taken from Grisales-Noreña et al. [24], Garces [25], Ocampo Toro [26], and Montoya et al. [27]. Given the simplicity of the conversion from radial to meshed, Table 2 only contains the information on the two lines added to the system. This procedure followed the recommendation by Ocampo Toro [26] and was also employed to obtain the meshed versions of the 33- and 69-node systems.

The meshed version of this system consists of 10 nodes and 11 lines, with base voltage and power of 1 kV and 100 kW.

3.2. 33-node test system

The radial version of this test system consists of 33 nodes and 32 lines. Its base voltage is 12.66 kV and its base power is 1000 kVA. Fig. 3 shows the electrical diagram of the system, and Table 3 lists its characteristics. The radial version of the 33-node system was adapted from Montoya et al. [27], [28].

To develop the meshed version of the 33-node system, three connection lines were added to the 33-node radial topology described above. Table 4 presents the information corresponding to the lines added to obtain the meshed system.

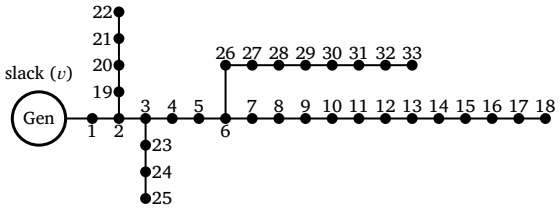

Fig. 3. 33-node radial topology.

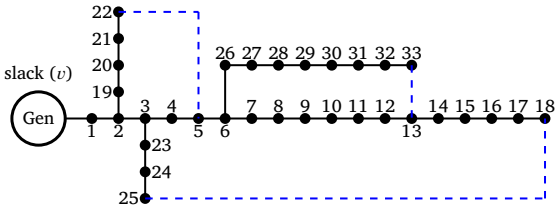

Fig. 4. 33-node meshed topology.

Table 3
Electrical parameters of the 33-node radial topology.

Node i	Node j	$R_{ij}[\Omega]$	$X_{ij}[\Omega]$	$P_j[kw]$	$Q_j[kVar]$
1	2	0.0922	0.0477	100	60
2	3	0.4930	0.2511	90	40
3	4	0.3660	0.1864	120	80
4	5	0.3811	0.1941	60	30
5	6	0.8190	0.7070	60	20
6	7	0.1872	0.6188	200	100
7	8	1.7114	1.2351	200	100
8	9	1.0300	0.7400	60	20
9	10	1.0400	0.7400	60	20
10	11	0.1966	0.0650	45	30
11	12	0.3744	0.1238	60	35
12	13	1.4680	1.1550	60	35
13	14	0.5416	0.7129	120	80
14	15	0.5910	0.5260	60	10
15	16	0.7463	0.5450	60	20
16	17	1.2890	1.7210	60	20
17	18	0.7320	0.5740	90	40
2	19	0.1640	0.1565	90	40
19	20	1.5042	1.3554	90	40
20	21	0.4095	0.4784	90	40
21	22	0.7089	0.9373	90	40
3	23	0.4512	0.3083	90	50
23	24	0.8980	0.7091	420	200
24	25	0.8960	0.7011	420	200
6	26	0.2030	0.1034	60	25
26	27	0.2842	0.1447	60	25
27	28	1.0590	0.9337	60	20
28	29	0.8042	0.7006	120	70
29	30	0.5075	0.2585	200	600
30	31	0.9744	0.9630	150	70
31	32	0.3105	0.3619	210	100
32	33	0.3410	0.5302	60	40

Table 4
Electrical parameters added to obtain the 33-node meshed topology.

Node i	Node j	$R_{ij}[\Omega]$	$X_{ij}[\Omega]$	$P_j[kw]$	$Q_j[kVar]$
5	22	1.4680	1.1550	90	40
18	25	0.5910	0.5260	420	200
13	33	1.5042	1.3554	60	40

The meshed version of the system consists of 33 nodes and 35 lines, and its base voltage and power are 12.66 kV and 1000 kVA, respectively. Fig. 4 presents the electrical diagram of the system, where the added lines are shown in blue. This test system was adapted from Montoya et al. [27], [28] and Kumar Sharma and Murty [29].

3.3. 69-node test system

The radial version of this test system consists of 69 nodes and 68 lines, its base voltage is 12.66 kV, and its base power is 1000 kVA. Fig. 5 presents the electrical configuration of the system, and Table 5 lists its technical parameters. This version of the 69-node test system was adapted from Montoya et al. [27], [28].

To develop the meshed topology, four connection lines were added to the 69-node radial system described above. Table 6 presents the

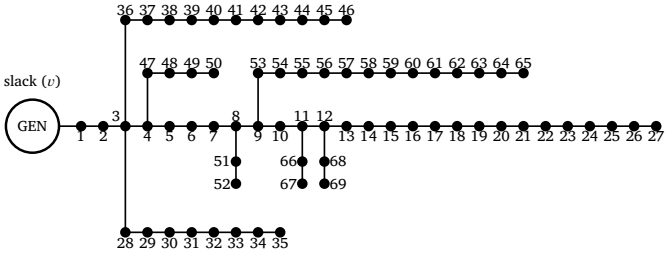

Fig. 5. 69-node radial topology.

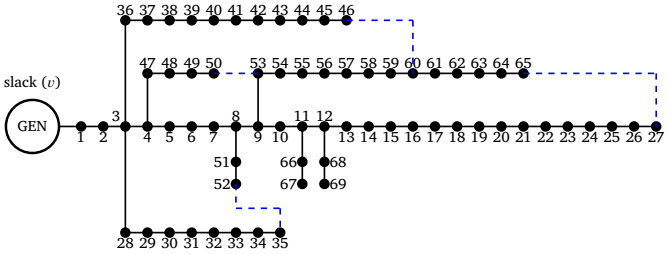

Fig. 6. 69-node meshed topology.

technical data corresponding to the lines added to obtain the meshed version of the system.

This meshed version consists of 69 nodes and 72 lines, its base voltage is 12.66 kV, and its base power is 1000 kVa. Fig. 6 presents the diagram of the system, where the new lines are shown in blue. This test system was proposed by Montoya et al. [27], [28] and Grisales-Noreña et al. [30].

3.4. Considerations

The following are the considerations that we took into account in this study for the comparative analysis of the selected solution methods:

- To analyze the convergence errors in terms of nodal voltages and power losses, we compared the average voltage errors obtained by each method with the values obtained by the NR method. NR was employed as the comparison method because, in the specialized literature, it has proven to converge to the solution of the LFP [3]. Therefore, it is used in the main simulation software packages, such as DIgSILENT, to validate load flows [31,32]. It is worth highlighting that, in this study, we obtained the voltage convergences of the solution methods by analyzing their average voltage errors with respect to those reported in the base case (NR), due to the space limitations of the paper. Regarding the power losses of each method, we analyzed the difference between the data obtained by the NR and the selected load flow methods in both radial and meshed topologies.
- As for the analysis of processing times, we collected the time obtained by each method and then we analyzed the time reduction percentage with respect to the NR method.

Table 5
Electrical parameters of the 69-node test system.

Node i	Node j	R_{ij} [Ω]	X_{ij} [Ω]	P[kW]	Q[kVar]	Node i	Node j	R_{ij} [Ω]	X_{ij} [Ω]	P[kW]	Q[kVar]
1	2	0.0005	0.0012	0	0	3	36	0.0044	0.0108	26	18.55
2	3	0.0005	0.0012	0	0	36	37	0.0640	0.1565	26	18.55
3	4	0.0015	0.0036	0	0	37	38	0.1053	0.1230	0	0
4	5	0.0215	0.0294	0	0	38	39	0.0304	0.0355	24	17
5	6	0.3660	0.1864	2.6	2.2	39	40	0.0018	0.0021	24	17
6	7	0.3810	0.1941	40.4	30	40	41	0.7283	0.8509	102	1
7	8	0.0922	0.0470	75	54	41	42	0.3100	0.3623	0	0
8	9	0.0493	0.0251	30	22	42	43	0.0410	0.0478	6	4.3
9	10	0.8190	0.2707	28	19	43	44	0.0092	0.0116	0	0
10	11	0.1872	0.0619	145	104	44	45	0.1089	0.1373	39.22	26.3
11	12	0.7114	0.2351	145	104	45	46	0.0009	0.0012	39.22	26.3
12	13	1.0300	0.3400	8	5	4	47	0.0034	0.0084	0	0
13	14	1.0440	0.3400	8	5	47	48	0.0851	0.2083	79	56.4
14	15	1.0580	0.3496	0	0	48	49	0.2898	0.7091	384.7	274.5
15	16	0.1966	0.0650	45	30	49	50	0.0822	0.2011	384.7	274.5
16	17	0.3744	0.1238	60	35	8	51	0.0928	0.0473	40.5	28.3
17	18	0.0047	0.0016	60	35	51	52	0.3319	0.1140	3.6	2.7
18	19	0.3276	0.1083	0	0	9	53	0.1740	0.0886	4.35	3.5
19	20	0.2106	0.0690	1	0.6	53	54	0.2030	0.1034	26.4	19
20	21	0.3416	0.1129	114	81	54	55	0.2842	0.1447	24	17.2
21	22	0.0140	0.0046	5	3.5	55	56	0.2813	0.1433	0	0
22	23	0.1591	0.0526	0	0	56	57	1.5900	0.5337	0	0
23	24	0.3463	0.1145	28	20	57	58	0.7837	0.2630	0	0
24	25	0.7488	0.2475	0	0	58	59	0.3042	0.1006	100	72
25	26	0.3089	0.1021	14	10	59	60	0.3861	0.1172	0	0
26	27	0.1732	0.0572	14	10	60	61	0.5075	0.2585	1244	888
3	28	0.0044	0.0108	26	18.6	61	62	0.0974	0.0496	32	23
28	29	0.0640	0.1565	26	18.6	62	63	0.1450	0.0738	0	0
29	30	0.3978	0.1315	0	0	63	64	0.7105	0.3619	227	162
30	31	0.0702	0.0232	0	0	64	65	1.0410	0.5302	59	42
31	32	0.3510	0.1160	0	0	65	66	0.2012	0.0611	18	13
32	33	0.8390	0.2816	10	10	66	67	0.0047	0.0014	18	13
33	34	1.7080	0.5646	14	14	67	68	0.7394	0.2444	28	20
34	35	1.4740	0.4873	4	4	68	69	0.0047	0.0016	28	20

Table 6
Electrical parameters added to obtain the 69-node meshed topology.

Node i	Node j	R_{ij} [Ω]	X_{ij} [Ω]	$P_j[kw]$	$Q_j[kVar]$
35	52	0.0022	0.0007	3.6	2.7
50	53	0.0057	0.0103	4.35	3.5
46	60	0.0275	0.0055	0	0
27	65	0.0025	0.1693	59	42

- The method with the lowest level of convergence errors and shortest processing time in both meshed and radial networks was selected as the most suitable method to solve the LFP.
- All the solution methods were assigned a convergence error (ϵ) of 1×1^{-10}, which was employed as the stopping criterion.
- To reduce the effect of other computational processes or interference in the processing times, the different test scenarios were executed 1×1^5 to identify the average processing time of each method [30].
- In order to ensure the proper comparison of the results, we conducted all the simulations on a Lenovo IdeaPad Gaming 3i laptop, with a 10th generation Intel Core i5-10300H processor, and a 12-GB RAM. In addition, we used MATLAB software to implement the load flow methods.

4. Simulation results

This section describes the simulation results of all the test systems employed in this study. The radial and meshed configurations were analyzed separately in order to identify the solution method with the best balance between convergence and processing time for the different topologies of the electrical systems selected.

4.1. Analysis of convergence and processing times in radial networks

We assessed the efficiency of the NR, GS, TS, SA, IS, and TM methods to solve the LFP in radial networks. To this end, we collected the power loss levels and processing times, which are detailed in Table 7. This table is divided into three columns that contain, from left to right, the solution method, the power losses of each method (in p.u), and the processing times required by each method. The table also comprises three subsections, which represent the three test scenarios (10, 33, and 69 nodes).

Table 8 lists the average voltage errors, the percentage power loss errors, and the time reductions obtained by each solution method in the radial systems, compared to the NR methodology. As for the nodal voltage errors, the table does not display the errors obtained by each of the nodes, but the average voltage error of the test system, considering the space limitations of this document and the extension of the data. Note that, in some cases, the time reduction values are negative; this is because the time did not decrease but increased when compared to the NR method.

According to Table 8, the highest value among the average voltage errors was obtained in the 69-node scenario, using the TS method (8.017×10^{-04}). However, it is an irrelevant error in terms of voltage, considering that, if we were working with kilovolts, this error would be in the volt range. Regarding the power losses in radial test systems, the scenario is similar. The largest error is found in the 69-node system using the GS method (5.613×10^{-07}). However, if the system were operating on the order of megawatts, this error would mean a difference of 0.1 watts, which is negligible due to the major difference between the errors and the working scales. Based on these results, we can conclude that all the numerical methods used in this study to solve the LFP in radial AC networks are suitable in terms of convergence.

With respect to the computation times, the GS method clearly displays the least favorable results, considering that it increases the time

Table 7
Power losses and processing times in radial networks.

Method	Power loss (p.u)	Processing time
10-node radial topology		
NR	2.23418140617546	0.350383
GS	2.23418140806228	0.889808
TS	2.23418140696487	0.135645
SA	2.23418140694496	0.084450
IS	2.23418140694527	0.108409
TM	2.23418140651530	0.035618
33-node radial topology		
NR	0.210978503766554	2.721391
GS	0.210978503038590	21.980785
TS	0.210978503766739	0.967009
SA	0.210978503761836	0.409485
IS	0.210978503761475	0.577689
TM	0.210978503707882	0.079691
69-node radial topology		
NR	0.225071470886112	9.404351
GS	0.225070909569565	136.555441
TS	0.225071470876815	2.989799
SA	0.225071470859690	1.940855
IS	0.225071470868345	2.352327
TM	0.225071470717744	0.185596

Table 8
Analysis of the different solution methods with respect to the NR method in the study of radial networks.

Method	Voltage error (p.u)	Loss error (p.u)	Time reduction (s)
10-node radial topology			
GS	1.674×10^{-10}	1.887×10^{-09}	-0.539
TS	4.144×10^{-12}	7.894×10^{-10}	0.215
SA	4.040×10^{-12}	7.695×10^{-10}	0.266
IS	4.041×10^{-12}	7.698×10^{-10}	0.242
TM	1.056×10^{-12}	3.397×10^{-10}	0.315
33-node radial topology			
GS	1.675×10^{-05}	7.280×10^{-10}	-19.259
TS	1.496×10^{-14}	1.850×10^{-13}	1.754
SA	6.722×10^{-13}	4.718×10^{-12}	2.312
IS	6.685×10^{-13}	5.079×10^{-12}	2.144
TM	8.082×10^{-12}	5.867×10^{-11}	2.642
69-node radial topology			
GS	2.896×10^{-05}	5.613×10^{-07}	-127.151
TS	8.017×10^{-04}	9.297×10^{-12}	6.415
SA	1.836×10^{-09}	2.642×10^{-11}	7.463
IS	1.836×10^{-09}	1.777×10^{-11}	7.052
TM	1.824×10^{-09}	1.684×10^{-10}	9.219

Table 9
Power losses and processing times in meshed networks.

Method	Power loss (p.u)	Processing time (s)
10-node meshed topology		
NR	1.90323657874833	0.356536
GS	1.90323657940136	1.453290
TS	1.90323657887076	0.123754
SA	1.90323657878735	0.076213
IS	1.90323657878838	0.156125
TM	1.90323657557859	0.047279
33-node meshed topology		
NR	0.159285326588047	2.737034
GS	0.159285326672570	35.33883
TS	0.159285326587817	0.965361
SA	0.159285326569052	0.327071
IS	0.159285326568758	1.138940
TM	0.159285326232904	0.152359
69-node meshed topology		
NR	0.0794264098676387	9.468824
GS	0.0794258034455151	780.4313
TS	0.0794264098279257	2.366148
SA	0.0794264098899297	1.441815
IS	0.0794264098677721	4.120223
TM	0.0794264097716617	0.464808

Table 10
Analysis of the different solution methods with respect to the NR method in the study of meshed networks.

Method	Voltage error (p.u)	Loss error (p.u)	Time reduction (s)
10-node meshed topology			
GS	6.431×10^{-10}	6.530×10^{-10}	-1.097
TS	6.529×10^{-13}	1.224×10^{-10}	0.233
SA	7.431×10^{-14}	3.902×10^{-11}	0.357
IS	7.431×10^{-14}	4.005×10^{-11}	0.200
TM	1.567×10^{-11}	3.170×10^{-09}	0.309
33-node meshed topology			
GS	1.702×10^{-06}	8.452×10^{-11}	-32.602
TS	5.090×10^{-15}	2.300×10^{-13}	1.772
SA	2.377×10^{-12}	1.900×10^{-11}	2.410
IS	2.373×10^{-12}	1.929×10^{-11}	1.598
TM	4.444×10^{-11}	3.551×10^{-10}	2.585
69-node meshed topology			
GS	1.488×10^{-06}	6.064×10^{-07}	-770.962
TS	3.963×10^{-04}	3.971×10^{-11}	7.103
SA	1.309×10^{-08}	2.229×10^{-11}	8.027
IS	1.309×10^{-08}	1.334×10^{-13}	5.349
TM	3.963×10^{-04}	9.598×10^{-11}	9.004

by -737.90%, compared to the NR method. As for the rest of the methods, we can observe reductions in the time required to solve the LFP, when compared to the NR method. The greatest reductions in processing times were achieved by the TM, followed by SA, IS, and TS in the last place. The results suggest that, as the number of nodes increases, the difference obtained by the methods in terms of processing times also grows. For example, if we analyze the performance of the TM, it achieved time reductions of 89.83% in the 10-node topology, 97.07% in the 33-node topology, and 98.03% in the 69-node topology, when compared with the NR method. Furthermore, when compared with the other methods, the TM obtained an average reduction of 76.91% in the 10-node system, 91.04% in the 33-node system, and 94.85% in the 69-node system. It means that its overall average improvement is 87.60% with respect to the processing times obtained by the other methods. Consequently, the TM is considered to be the most efficient method in terms of processing time when analyzing different sizes of radial AC networks.

4.2. Analysis of convergence and processing times in meshed networks

In this section, to assess the efficiency of the solution in meshed networks, we considered the same methods as in Section 4.1. The results of the performance analysis of these methods are summarized in Table 9, which presents the same structure as Table 7.

In order to use the same structure in the different analyses described throughout the document and present the information homogeneously, Table 10 lists the performance of the solution methods in the same way as Table 8. In this case, the NR method is also used as the comparison method.

According to the average voltage errors shown in Table 8, the highest error is found in the 69-node topology when using the TS method (3.963×10^{-04}). Regarding power losses, the largest error is found in the 69-node system when the GS method is employed (6.064×10^{-07}). Based on the previous results, we can infer that, like in radial networks, all the methods studied are suitable in terms of convergence to solve the LFP in meshed AC networks.

In terms of computation times, we can clearly observe that, again, the GS method presents the least favorable results. When compared to the NR method, it increases the processing time by -3213.62%, unlike the rest of the methods that reduce it. The TM method offers the greatest reductions in processing times, followed by SA, TS, IS, and GS in comparison with the NR methodology. Specifically, it reduced the processing time by 86.74% in the 10-node topology, by 94.43% in the 33-node topology, and by 95.09% in the 69-node topology. Additionally, when compared to the other methods, TM achieved an average reduction of 70.59% in the 10-node system, 83.65% in the 33-node system, and 86.37% in the 69-node system. It also exhibited an overall average improvement of 80.21% with respect to the other solution methods. This demonstrates that, in terms of processing times, TM is the most efficient method to solve the LFP in meshed AC networks.

4.3. Analysis of the load flow methods in radial and meshed networks

This section only analyzes the processing times because, as explained above, the convergence errors in both radial and meshed networks are not significant enough to be considered as a selection criterion. Therefore, in terms of convergence, all the methods under study are suitable for solving the LFP in radial and meshed AC networks. In contrast, the processing times of the different methods do differ substantially, which makes it a crucial criterion when selecting a method to solve the LFP. The best method in terms of processing times was TM, which, in comparison with the other methods, reached overall average reductions of 87.60% and 80.21% for the radial and meshed networks, respectively. It is worth mentioning that the topology of a network can change under real operating conditions due to the activation of disconnectors or protective devices entrusted with recovering electrical zones under faults. Therefore, it is essential to identify a method that can solve the LFP in both meshed and radial networks while ensuring short processing times. Based on these conditions and given its short processing times, this study concludes that TM is the method of choice.

5. Conclusions

As explained in previous sections, the LFP in AC networks is a nonlinear and non-convex problem that must be solved using numerical methods. Although this problem is not new, a literature review allowed us to determine that it still prevails due to the need to optimize the management and planning of electrical networks to ensure short response times, thus minimizing the environmental impacts and operating costs of the existing electrical systems.

From this study, we concluded that all the methods selected to solve the LFP in AC networks offer excellent results in terms of convergence, considering that the greatest errors were 6.064×10^{-07} for power losses and 8.017×10^{-04} for nodal voltages, which are negligible values for practical purposes. Therefore, the key factor when selecting a solution method for the LFP is the processing time since an unsuitable method can imply processing times up to 541.283 times longer.

Based on the results obtained in this research, it is recommended that the TM method be used when solving the LFP problem, as it exhibited overall average processing time reductions of 87.60% and 80.21% in radial and meshed networks, respectively, *i.e.*, in comparison with the other solution methods analyzed. Its efficiency is such that the next most efficient method (SA) is 498.89% slower on average at solving radial networks. Thereupon, TM is the best method for solving the LPF in both topologies, which is fundamental in the management and planning of electrical networks, as it is common for networks to change their topology during operation due to protector and disconnector devices.

Future lines of research might include the analysis and implementation of new numerical methods to solve the LFP in electrical systems to ensure convergence and improve the computation times reported in the specialized literature. Another possible application of the results obtained in this paper is to propose strategies to plan and operate power systems using the load flow methods selected here for the different topologies. This would allow researchers to explore solution spaces in a suitable way, with short processing times.

CRediT authorship contribution statement

All authors of this manuscript worked on the conceptualization, methodology, software, validation, formal analysis, investigation, resources, data curation, writing – original draft, writing – review & editing, visualization, supervision, project administration, and funding acquisition.

Declaration of competing interest

The authors declare that they have no known competing financial interests or personal relationships that could have appeared to influence the work reported in this paper.

Data availability

Data will be made available on request.

Acknowledgement

This research was funded by the Universidad de Talca-Chile, Instituto Tecnológico Metropolitano-Colombia, Universidad Distrital Francisco José de Caldas-Colombia y la Universidad Tecnológica de Pereira-Colombia.

References

[1] O.D. Montoya, A. Molina-Cabrera, D.A. Giral-Ramírez, E. Rivas-Trujillo, J.A. Alarcón-Villamil, Optimal integration of D-STATCOM in distribution grids for annual operating costs reduction via the discrete version sine-cosine algorithm, Results Eng. 16 (2022) 100768, https://doi.org/10.1016/j.rineng.2022.100768.

[2] F. Capitanescu, Critical review of recent advances and further developments needed in ac optimal power flow, Electr. Power Syst. Res. 136 (2016) 57–68.

[3] O.D. Montoya, V.M. Garrido, W. Gil-González, L.F. Grisales-Noreña, Power flow analysis in dc grids: two alternative numerical methods, IEEE Trans. Circuits Syst. II, Express Briefs 66 (11) (2019) 1865–1869.

[4] J. Montano, O.D. Garzón, A.A.R. Muñoz, L. Grisales-Noreña, O.D. Montoya, Application of the arithmetic optimization algorithm to solve the optimal power flow problem in direct current networks, Results Eng. 16 (2022) 100654.

[5] I. Diahovchenko, R. Petrichenko, L. Petrichenko, A. Mahnitko, P. Korzh, M. Kolcun, Z. Čonka, Mitigation of transformers' loss of life in power distribution networks with high penetration of electric vehicles, Results Eng. 15 (2022) 100592.

[6] S. Huang, Q. Wu, J. Wang, H. Zhao, A sufficient condition on convex relaxation of ac optimal power flow in distribution networks, IEEE Trans. Power Syst. 32 (2) (2016) 1359–1368.

[7] M. John, A general method of digital network analysis particularly suitable for use with low-speed computers, Proceedings of the IEE-Part A: Power Engineering 108 (41) (1961) 369–382.

[8] M. Laughton, M.H. Davies, Numerical Techniques in Solution of Power-System Load-Flow Problems, Proceedings of the Institution of Electrical Engineers, vol. 111, IET, 1964, pp. 1575–1588.

[9] A. Vijayvargia, S. Jain, S. Meena, V. Gupta, M. Lalwani, Comparison between different load flow methodologies by analyzing various bus systems, Int. J. Electr. Eng. 9 (2) (2016) 127–138.

[10] M.L. Manrique, O.D. Montoya, V.M. Garrido, L.F. Grisales-Noreña, W. Gil-González, Sine-cosine algorithm for opf analysis in distribution systems to size distributed generators, in: Workshop on Engineering Applications, Springer, 2019, pp. 28–39.

[11] H.F. Farahani, A. Kazemi, S. Hosseini, A new algorithm for identifying branch and node after any bus to use load-flow in radial distribution systems, in: 2007 42nd International Universities Power Engineering Conference, IEEE, 2007, pp. 1129–1133.

[12] O.D. Montoya, On linear analysis of the power flow equations for dc and ac grids with cpls, IEEE Trans. Circuits Syst. II, Express Briefs 66 (12) (2019) 2032–2036.
[13] L.F. Grisales, B.J. Restrepo Cuestas, et al., Ubicación y dimensionamiento de generación distribuida: Una revisión, Ciencia e Ingeniería Neogranadina 27 (2) (2017) 157–176.
[14] K. López-Rodríguez, W. Gil-González, A. Escobar-Mejía, Design and implementation of a pi-pbc to manage bidirectional power flow in the dab of an sst, Results Eng. (2022) 100437.
[15] C.A.P. Meneses, J.R.S. Mantovani, Improving the grid operation and reliability cost of distribution systems with dispersed generation, IEEE Trans. Power Syst. 28 (3) (2013) 2485–2496.
[16] J.J. Grainger, W.D. Stevenson, Power systems analysis, 1996.
[17] O.D. Montoya, A. Molina-Cabrera, J.C. Hernández, A comparative study on power flow methods applied to ac distribution networks with single-phase representation, Electronics 10 (21) (2021) 2573.
[18] J.-H. Teng, A modified Gauss–Seidel algorithm of three-phase power flow analysis in distribution networks, Int. J. Electr. Power Energy Syst. 24 (2) (2002) 97–102.
[19] J.-H. Teng, A direct approach for distribution system load flow solutions, IEEE Trans. Power Deliv. 18 (3) (2003) 882–887.
[20] O.D. Montoya, L.F. Grisales-Noreña, W. Gil-González, Triangular matrix formulation for power flow analysis in radial dc resistive grids with cpls, IEEE Trans. Circuits Syst. II, Express Briefs 67 (6) (2019) 1094–1098.
[21] A. Marini, S. Mortazavi, L. Piegari, M.-S. Ghazizadeh, An efficient graph-based power flow algorithm for electrical distribution systems with a comprehensive modeling of distributed generations, Electr. Power Syst. Res. 170 (2019) 229–243.
[22] W. Wu, B. Zhang, A three-phase power flow algorithm for distribution system power flow based on loop-analysis method, Int. J. Electr. Power Energy Syst. 30 (1) (2008) 8–15.
[23] S.Y. Bocanegra, W. Gil-González, O.D. Montoya, A new iterative power flow method for ac distribution grids with radial and mesh topologies, in: 2020 IEEE International Autumn Meeting on Power, Electronics and Computing (ROPEC), vol. 4, IEEE, 2020, pp. 1–5.
[24] L.F. Grisales-Noreña, O.D. Montoya, C.A. Ramos-Paja, Q. Hernandez-Escobedo, A.-J. Perea-Moreno, Optimal location and sizing of distributed generators in dc networks using a hybrid method based on parallel pbil and pso, Electronics 9 (11) (2020) 1808.
[25] A. Garces, Uniqueness of the power flow solutions in low voltage direct current grids, Electr. Power Syst. Res. 151 (2017) 149–153.
[26] J.A. Ocampo Toro, Despacho optimo de potencia en microrredes de corriente continua considerando variacion en la generacion eolica y solar y el comportamiento de demanda de energia, 2021.
[27] O.D. Montoya, W. Gil-González, D.A. Giral, On the matricial formulation of iterative sweep power flow for radial and meshed distribution networks with guarantee of convergence, Appl. Sci. 10 (17) (2020) 5802.
[28] O.D. Montoya, W. Gil-González, L. Grisales-Noreña, An exact minlp model for optimal location and sizing of dgs in distribution networks: a general algebraic modeling system approach, Ain Shams Eng. J. 11 (2) (2020) 409–418.
[29] A. Kumar Sharma, V. Murty, Analysis of mesh distribution systems considering load models and load growth impact with loops on system performance, J. Inst. Eng. (India), Ser. B 95 (4) (2014) 295–318.
[30] L.F. Grisales-Noreña, O.D. Montoya, W.J. Gil-González, A.-J. Perea-Moreno, M.-A. Perea-Moreno, A comparative study on power flow methods for direct-current networks considering processing time and numerical convergence errors, Electronics 9 (12) (2020) 2062.
[31] R. Villena-Ruiz, A. Honrubia-Escribano, J. Fortmann, E. Gómez-Lázaro, Field validation of a standard type 3 wind turbine model implemented in digsilent-powerfactory following iec 61400-27-1 guidelines, Int. J. Electr. Power Energy Syst. 116 (2020) 105553.
[32] D.L. Bernal-Romero, O.D. Montoya, A. Arias-Londoño, Solution of the optimal reactive power flow problem using a discrete-continuous cbga implemented in the digsilent programming language, Computers 10 (11) (2021) 151.